

THE OPTICAL APPROACH TO CASIMIR EFFECTS

A. SCARDICCHIO*

*Center for Theoretical Physics,
Laboratory for Nuclear Science and Department of Physics
Massachusetts Institute of Technology
Cambridge, MA 02139, USA*

We propose a new approach to the Casimir effect based on classical ray optics. We define and compute the contribution of classical optical paths to the Casimir force between rigid bodies. Our approach improves upon the proximity force approximation. It can be generalized easily to arbitrary geometries, different boundary conditions, to the computation of Casimir energy densities and to many other situations.

MIT-CTP-3522

1. Introduction

The last 10 years have witnessed quite a revolution in the experimental techniques used to prove Casimir effect.¹ Casimir's original prediction for the force between grounded conducting plates due to modifications of the zero point energy of the electromagnetic field has already been verified to an accuracy of a few percent. Progress has been slower on the theoretical side. Beyond Casimir's original study of parallel plates,² we are only aware of useful calculations for a corrugated plate³ and for a sphere and a plate.⁴ Simple and experimentally interesting geometries like two spheres, a finite inclined plane opposite an infinite plane, and a pencil point and a plane, remain elusive. The Proximity Force Approximation⁵ (PFA) was shown by Gies *et al.*⁴ to deviate significantly from their precise numerical result for the sphere and plane. Thus at present neither exact results nor reliable approximations are available for generic geometries. It was in this context that we recently proposed a new approach to Casimir effects based on classical optics.⁶ The basic idea is extremely simple: first the Casimir energy

*Joint work with R. L. Jaffe

is recast as a trace of the Green's function; then the Green's function is approximated by the sum over contributions from optical paths labelled by the number of (specular) reflections from the conducting surfaces. The integral over the wave numbers of zero point fluctuations can be performed analytically, leaving a formula which depends only on the properties of the paths between the surfaces. This approach will give an approximation (though a surprisingly accurate one) which is valid when the natural scales of diffraction are large compared to the scales that measure the strength of the Casimir force. In practice this will typically be measured by the ratio of the separation between the conductors, a , to their curvature, R . It generalizes naturally to the study of Casimir thermodynamics, energy and pressure, to various b.c., to fermions, and to compact and/or curved manifolds.

In the optical approximation the cutoff dependent terms of the Casimir energy can easily be isolated and shown to be independent of the separation between conductors. They therefore do not contribute to forces and can be dropped.

2. Derivation

Most studies of Casimir energies do not consider approximations. Instead they focus on ways to regulate and compute the sum over modes, $\sum \frac{1}{2}\hbar\omega$.⁷ These methods have proved very difficult to apply to geometries other than parallel plates. The main reason for this *impasse* lies in the requirement of an analytic knowledge of the spectrum of the Laplace operator for the given geometry. However, the knowledge of this spectrum for a family of boundaries (like a sphere facing a plane) would have the most non-trivial implications for the same family of quantum billiards and hence of classical billiards. 30 years of work on the ergodicity of classical billiards and their quantum counterparts suggest this task is hopeless.⁸

A numerical knowledge of the spectrum does not represent a reliable solution to the problem either. The force, indeed, is given by the small oscillatory ripple in the density of state numerically shadowed by the 'bulk' contributions which give rise to distance-independent divergencies.

So we focused our attention on ways to get approximate solutions of the Laplace-Dirichlet problem which are apt to capture the oscillatory contributions in the density of states, providing physical insights and accurate numerical estimates.

2.1. The Optical Approximation for the propagator

There is a strong connection between the Casimir energy for a field ϕ obeying Dirichlet boundary conditions (b.c.) on the boundary of the domain D and the propagator $G(x', x, k)$ of the Helmholtz equation on the same domain with the same b.c. . The knowledge of the latter allows one to calculate the density of states $\rho(k)$ and from this we can obtain the Casimir energy by quadratures. Indeed, from the well-known definition of the Casimir energy in terms of a space and wave-number dependent density of states,⁹ $\rho(x, k)$,

$$E_D[\phi] = \int_0^\infty dk \int_D d^N x \frac{1}{2} \hbar \omega(k) \rho(x, k), \quad (2.1)$$

where $\omega(k) = c\sqrt{k^2 + \mu^2}$, and the density of states $\rho(x, k)$ is related to the propagator $G(x', x, k)$ by

$$\rho(x, k) = \frac{2k}{\pi} \text{Im } G(x, x, k). \quad (2.2)$$

where the usual density of states is $\rho(k) = \int d^N x \rho(x, k)$.

We must choose G to be analytic in the upper-half k^2 -plane; in the time domain (see later) this means we are taking the retarded propagator.

The Casimir energy depends on the b.c. obeyed by the field ϕ and on the arrangement of the boundaries, $S \equiv \partial D$ (not necessarily finite), of the domain D . From the outset we recognize that E must be regulated, and will in general be cutoff dependent. We will not denote the cutoff dependence explicitly except when necessary. ρ and G are the familiar density of states and propagator associated with the problem

$$(\Delta + k^2)\psi(x) = 0 \quad \text{for } x \in D, \quad \psi(x) = 0 \quad \text{for } x \in S. \quad (2.3)$$

We can regard this problem as the study of a quantum mechanical free particle with $\hbar = 1$, mass $m = 1/2$, and energy $E = k^2$, living in the domain D with Dirichlet b.c. on ∂D . Dirichlet b.c. are an idealization for the interactions which prevent the quantum particle from penetrating beyond the surfaces S . This is adequate for low energies but fails for the divergent, *i.e.* cutoff dependent, contributions to the Casimir energy.¹⁰ However, the divergences can be simply disposed of in the optical approach, and the physically measurable contributions to Casimir effect are dominated by $k \sim 1/a$, where a , a typical plate separation, satisfies $1/a \ll \Lambda$ with Λ being the momentum cutoff characterizing the material. So the boundary conditions idealization is quite adequate for our purposes. Following this

quantum mechanics analogy we introduce a fictitious time, t , and consider the functional integral representation of the propagator.¹¹ The space-time propagator $G(x', x, t)$ obeys the free Schrödinger equation in D bounded by S . It can be written as a functional integral over paths from x' to x with action $S(x', x, t) = \frac{1}{4} \int_0^t dt \dot{x}^2$. The optical approximation is obtained by taking the stationary phase approximation of the propagator G in the fictitious time domain

$$G_{\text{opt}}(x', x, t) = \sum_r K_r(x', x, t) e^{iS_r(x', x, t)}. \quad (2.4)$$

The classical action is

$$S_r(x', x, t) = \frac{\ell_r(x', x)^2}{4t} \quad (2.5)$$

and K_r is the van Vleck determinant

$$K_r(x', x, t) \propto \det \left(\frac{\partial^2 \ell_r^2}{\partial x'_i \partial x_j} \right)^{1/2}. \quad (2.6)$$

With some manipulations⁶ we can turn this determinant into

$$K_r(x', x, t) = \frac{(-1)^r}{(4\pi it)^{N/2}} \left(\ell_r^{N-1} \frac{d\Omega_x}{dA'_x} \right)^{1/2}, \quad (2.7)$$

where N is the number of spatial dimensions. This approximation is exact to the extent one can assume the classical action of the path S_r to be quadratic in x', x . This is the case for flat and infinite plates. Thus the non-quadratic part of the classical action comes from the curvature or the finite extent of the boundaries, which we parameterize generically by R , $\partial^3 S / \partial x^3 \sim 1/Rt$.

In k -space the corrections hence will be $O(1/kR)$, and the important values of k for the Casimir energy are of order $1/a$, where a is a measure of the separation between the surfaces. Thus the figure of merit for the optical approximation is a/R . Certainly some of the curvature effects are captured by the van Vleck determinant but at the moment there is no good way to estimate the order in a/R of the corrections to the optical approximation (possibly fractional, plus exponentially small terms). This is topic for further investigation.

Putting all together we find the space-time form of the optical propagator to be

$$G_{\text{opt}}(x', x, t) = \sum_r \frac{(-1)^r}{(4\pi it)^{N/2}} \left(\ell_r^{N-1} \frac{d\Omega_x}{dA'_x} \right)^{1/2} e^{i\ell_r^2/4t}. \quad (2.8)$$

When dealing with infinite, parallel, flat plates this approximation becomes exact. For a single infinite plate, for example, the length-squared of the only two paths going from x to x' are $\ell_{\text{direct}}^2 = ||x' - x||^2$, $\ell_{\text{reflection}}^2 = ||x' - \tilde{x}||^2$, where \tilde{x} is the image of x . Both are quadratic functions of the points x, x' and the optical approximation is indeed exact. $G_{\text{opt}}(x', x, k)$ is obtained by Fourier transformation and can be expressed in terms of Hankel functions, giving us the final form for our approximation

$$\begin{aligned} G_{\text{opt}}(x', x, k) &= \sum_r \frac{(-1)^r i \pi}{(4\pi)^{N/2}} (\ell_r^{N-1} \Delta_r)^{1/2} \left(\frac{\ell_r}{2k} \right)^{1-N/2} H_{\frac{N}{2}-1}^{(1)}(k\ell_r), \\ &\equiv \sum_r G_r(x', x, k), \end{aligned} \quad (2.9)$$

where Δ_r is the enlargement factor (see⁶ for details)

$$\Delta_r(x', x) = \frac{d\Omega_x}{dA_{x'}} \quad (2.10)$$

and we have suppressed the arguments x and x' on ℓ_r and Δ_r in (2.9). This can be thought of as a particular case of a more general result.¹²

2.2. The Optical Casimir energy

The substitution of (2.9) into (2.2) and then in (2.1) gives rise to a series expansion of the Casimir energy associated with classical closed (but not necessarily periodic) paths

$$E_{\text{opt}} = \sum_{\text{paths } r} E_r, \quad (2.11)$$

where each term of this series will be in the form of

$$E_r = \frac{1}{2} \hbar \text{Im} \int_0^\infty dk \omega(k) \frac{2k}{\pi} \int_{D_r} d^N x G_r(x, x, k). \quad (2.12)$$

Here the integration has been restricted to the domain $D_r \subset D$ where the given classical path r exists. If the length of the path is bounded from below (this is the case for more than one reflection) the x and k integral can be switched safely. The k -integral can be performed exactly for any N and μ , but it is particularly simple for the massless case, $\omega(k) = ck$,

$$E_r = \hbar c \frac{(-1)^{r+1}}{2\pi^{N/2+1/2}} \Gamma\left(\frac{N+1}{2}\right) \int_{D_r} d^N x \frac{\Delta_r^{1/2}}{\ell_r^{(N+3)/2}}. \quad (2.13)$$

This is the central result of our work and associates a Casimir energy contribution to each optical path $r > 1$. The series (2.11) has a very fast

convergence, usually 98% of the contribution is contained in the first 4 terms, as we will see in the examples below.

2.3. Divergencies

The paths $r = 1B$ that bounce only once on a given body B must be treated with particular care because their contribution is divergent. The x and k integrals cannot be inverted without regulating the divergencies. To do so we insert a simple exponential cutoff in k . For a massless field the k -integration in E_{1B} can be performed^a giving

$$E_{1B} = -\frac{\hbar c}{4\pi^2} \int_{D_{1B}} d^3x \Delta_{1B}^{1/2} \frac{2\ell_{1B}\Lambda^4(3 - (\ell_{1B}\Lambda)^2)}{(1 + (\ell_{1B}\Lambda)^2)^3}. \quad (2.14)$$

Notice that for $\ell_{1B}\Lambda \gg 1$ we reobtain the standard result, eq. (2.13). Hence it is convenient to rewrite this integral as

$$E_{1B} = -\frac{\hbar c}{4\pi^2} \left(\int_{D_{1B} \cup \overline{D}_{1B}} d^3x - \int_{\overline{D}_{1B}} d^3x \right) \Delta_{1B}^{1/2} \frac{2\ell_{1B}\Lambda^4(3 - (\ell_{1B}\Lambda)^2)}{(1 + (\ell_{1B}\Lambda)^2)^3}, \quad (2.15)$$

where \overline{D}_{1B} is the domain where the path *does not* exist. The first integral does not depend on the position of the other bodies and in the second we can take the limit $\Lambda \rightarrow \infty$ safely because $\ell_{1B}(x) > 2a > 0$, where a is the minimum distance between the bodies. Hence we will write $E_{1B} = E_{1B,\text{div}} + E_{1B,\text{fin}}$, the finite part being the integral over \overline{D}_{1B} (notice the extra minus sign).

The first term contains all the divergencies arising for $\ell_{1B} \rightarrow 0$. Notice that since when $\ell_{1B}\Lambda = \sqrt{3}$ the *sign* of the integrand changes, the divergence is negative rather than positive, as one could have argued from (2.13).¹⁵ Of course the bulk contribution to the vacuum fluctuation energy comes from the zero-reflection term, which is positive.

Using the expression of Δ_{1B} for a general surface with principal radii of curvature $R_{a,b}$ we find

$$E_{1B,\text{div}} \sim -\frac{S}{8\pi} \hbar c \Lambda^3 - \Lambda^2 \frac{1}{32\pi^2} \hbar c \int dS \left(\frac{1}{R_a} + \frac{1}{R_b} \right) + O(\ln \Lambda). \quad (2.16)$$

These terms do not contribute to the forces between rigid objects. The form of eq. (2.16) invites comparison with the work of Balian and Bloch.¹³ One finds agreement in the surface terms but not in the curvature terms.

^aFor simplicity we specialize to $N = 3$ although the analysis is completely general.

3. Parallel Plates

Parallel plates provide a simple, pedagogical example which has many features — fast convergence, trivial isolation of divergences, dominance of the even reflections — that occur in all the geometries we analyzed. We assume for simplicity that the two plates have the same area S . The relevant paths are shown in Fig. 1 where the points x and x' , which should be equal, are separated for ease of viewing. For the even paths $\ell_{2n}(z) = 2na$, $n = 1, 2, \dots$, independent of z (here z is the distance from the lower surface). For the odd paths $\ell_{2n-1,\alpha}(z) = 2(n-1)a + 2\zeta$, where $\zeta = z, a - z$ respectively if $\alpha = \text{down, up}$ and $n = 1, 2, \dots$. For planar boundaries the enlargement factor is given by $\Delta_{\mathbf{n}} = 1/\ell_{\mathbf{n}}^2$.

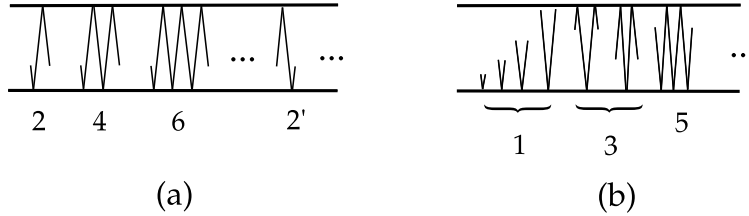


Figure 1. a) Even and b) odd optical paths for parallel plates. Initial and final points have been separated for visibility.

The sum over even reflections,

$$E_{\text{even}} = -\frac{\hbar c}{\pi^2} \sum_{n=1}^{\infty} \int dS \int_0^a dz \frac{1}{(2na)^4} = -\frac{\pi^2 \hbar c}{1440 a^3} S \quad (3.17)$$

is trivial because it is independent of z . The result is the usual Dirichlet Casimir energy.¹ The sum over odd reflections, after being regulated by point splitting, before removing the infinite part, gives

$$E_{\text{odd}} = \frac{\hbar c}{2\pi^2} \int dS \sum_{n=0}^{\infty} \int_0^a dz \frac{1}{(\epsilon^2 + (2z + 2na)^2)^2} = \frac{\hbar c}{16\pi^2} \frac{2\pi S}{\epsilon^3}. \quad (3.18)$$

The divergence as $\epsilon \rightarrow 0$ is precisely what is expected on the basis of the general analysis of the density of states in domains with boundaries.^{13,14} Moreover, since it is independent of a , it does not give rise to a force. From Fig. 1 b) it is evident why this must happen. The total sum of the off reflection contributions is just the integral of the one reflection path extended to ∞ and hence does not depend on a .

The fact that the odd reflections sum up to a divergent constant is universal for geometries with planar boundaries, and to a good approximation is also valid for curved boundaries. Note also that the sum over n in eq. (3.17), converges rapidly: 92% of the effect comes from the first term (the two reflection path) and $> 98\%$ comes from the two and four reflection paths. This rapid convergence persists for all the geometries we have analyzed due to the rapid increase in the length of the paths.

4. Sphere and Plane

We calculated the Casimir energy for the sphere and the plane up to four reflections. E_1 and E_3 can be found analytically while E_2 and E_4 must be computed numerically. Henceforth a will be the distance between the sphere and the plate and R the radius of the sphere.

Comparison with the parallel plate case as $a \rightarrow 0$ suggests the error due to neglecting the fifth and higher reflections to be $\sim 2\%$. Hence we have plotted our results as a band 2% in width in Fig. 2. Since the fractional contribution of higher reflections decreases with a , we believe this is a conservative estimate for larger a .

The proximity force approximation has been the standard tool for estimating the effects of departure from planar geometry for Casimir effects for many years⁷. In this approach one views the sphere and the plate as a superposition of infinitesimal parallel plates (i.e. the sphere is substituted by a stairlike surface). The resulting expression is

$$E_{\text{PFA}}^{\text{plate}} = -\frac{\pi^3 \hbar c R}{1440 a^2} \frac{1}{1 + a/R}. \quad (4.19)$$

It is custom to factor out the most divergent term of the Casimir *force* in the limit $a/R \rightarrow 0$ as predicted by the PFA, in this case $-\pi^3 \hbar c R / 720 a^3$, so to write in general

$$F = -f\left(\frac{a}{R}\right) \frac{\pi^3 \hbar c R}{720 a^3}, \quad (4.20)$$

which is the definition of f . Modern experiments are approaching accuracies where the deviations of $f(a/R)$ from unity are important. PFA predicts that

$$f_{\text{PFA}}(a/R) = 1 - \frac{1}{2} \frac{a}{R} + O\left(\frac{a^2}{R^2}\right), \quad (4.21)$$

while the optical approximation data predict

$$f_{\text{optical}}(a/R) = 1 + 0.05 \frac{a}{R} + O\left(\frac{a^2}{R^2}\right). \quad (4.22)$$

Beyond the limit of small a/R , one must notice that the optical approximation to the Casimir energy and the data of Ref. ⁴ both fall like $1/a^2$ at large a/R . In fact both are roughly proportional to $1/a^2$ for all a . In contrast the PFA estimates of the energy falls like $1/a^3$ at large a and departs from the Gies *et al.*⁴ data at relatively small a/R . For purposes of display we therefore scale the estimates of the energy by the factor $-1440a^2/\pi^3 R \hbar c$. The results are shown in Fig. 2. The dominant contri-

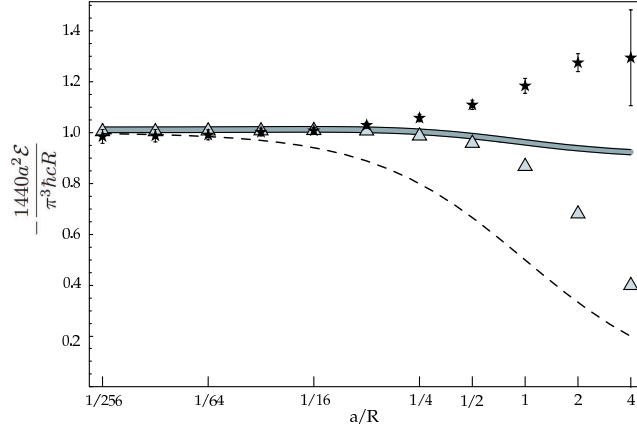


Figure 2. Sphere facing a plane case. Comparison between different methods. Results for Ref.4 (stars with error bars), data from 6, superseded by this work (triangles), optical approximation (thick grey line), PFA (broken line).

bution, always greater than 92%, comes from the second reflection. The fourth reflection contributes about 6% for $a/R \ll 1$ and less as a/R increases. The contributions of the first and third reflections are very small for all a/R . A relevant result, confirmed by the analytical analysis on the energy momentum tensor (within the optical approximation¹⁶) is that the asymptotic behavior of E as $a/R \gg 1$ predicted by the optical approximation is $\propto 1/a^2$. This is in contrast with the Casimir-Polder law which predicts $E \propto 1/a^4$ at large a , the discrepancy is to be attributed to settling in of diffraction effects.

5. Conclusions

We have proposed a new method for calculating approximately Casimir energies between conductors in generic geometries. We use an approximation imported from studies of wave optics that we have therefore named the

“optical approximation”. In this paper, we have outlined the derivation and applied it to two examples: the canonical example of parallel plates and the experimentally relevant situation of a sphere facing a plane. Our results are in agreement with the Proximity Force Approximation only to leading order in the small distances expansion. The first order correction is found to be different. This is of particular importance in the example of the sphere and the plane because the first order correction in a/R (a is the distance sphere-plate and R is the radius of the sphere) will soon be measured by new precision experiments.

We would like to thank the organizers of the conference ‘Continuous Advances in QCD 2004’. This work is supported in part by the U.S. Department of Energy (D.O.E.) under cooperative research agreement #DF-FC02-94ER40818 and in part by the INFN-MIT ‘Bruno Rossi’ fellowship.

References

1. S. K. Lamoreaux, Phys. Rev. Lett. **78**, 5 (1997); M. Bordag, U. Mohideen and V. M. Mostepanenko, Phys. Rept. **353**, 1 (2001); G. Bressi, G. Carugno, R. Onofrio and G. Ruoso, Phys. Rev. Lett. **88**, 041804 (2002); R. S. Decca, E. Fischbach, G. L. Klimchitskaya, D. E. Krause, D. L. Lopez and V. M. Mostepanenko, Phys. Rev. D **68**, 116003 (2003).
2. H. B. G. Casimir, Proc. K. Ned. Akad. Wet. **51**, 793 (1948).
3. R. Golestanian and M. Kardar, Phys. Rev. A **58**, 1713 (1998).
4. H. Gies, K. Langfeld and L. Moyaerts, JHEP **0306**, 018 (2003).
5. B. V. Derjagin, Kolloid Z. **69** 155 (1934).
6. R. L. Jaffe and A. Scardicchio, Phys. Rev. Lett. **92**, 070402 (2004); A. Scardicchio and R. L. Jaffe, [arXiv:quant-ph/0406041].
7. V. M. Mostepanenko and N. N. Trunov, *Casimir Effect and Its Applications*, Oxford University Press, (1997).
8. M. C. Gutzwiller, J. Math. Phys. **12**, 343 (1971); *Chaos in Classical and Quantum Mechanics*, Springer, Berlin (1990).
9. For a discussion, see Appendix A in Ref. ¹⁵.
10. N. Graham, R. L. Jaffe, V. Khemani, M. Quandt, O. Schroeder and H. Weigel, Nucl. Phys. B **677**, 379 (2004).
11. L. S. Schulman, *Techniques and Applications of Path Integration*, John Wiley & Sons; (1981).
12. M. V. Berry and K. E. Mount, Reps. Prog. Phys **35**, 315 (1972).
13. R. Balian and C. Bloch, Annals Phys. **69**, 401 (1970); **63**, 592 (1971); **69**, 76 (1972).
14. D. Deutsch and P. Candelas, Phys. Rev. D **20**, 3063 (1979).
15. N. Graham, R. L. Jaffe, V. Khemani, M. Quandt, M. Scandurra and H. Weigel, Nucl. Phys. B **645**, 49 (2002).
16. A. Scardicchio, R. L. Jaffe, to be published.